Electronic Supplementary Material (ESI) for Journal of Materials Chemistry A.

Supporting Information

Diatomic Molecule Catalysts toward Synergistic Electrocatalytic Carbon Dioxide Reduction

Liming Hong, Xian Liu, Baozhu Chi, Guomin Xia, Hongming Wang*

College of Chemistry and Institute for advanced Study, Nanchang University, Nanchang 330031, China

E-mail: hongmingwang@ncu.edu.cn

Supplementary Index

Table S1. CO_2RR performance comparison of different catalysts for CO production

Catalyst	Electrolyte	Potential (V *vs.* RHE)	CO product FE (%)	Stability (h)	Ref
D-Co	0.5 M $KHCO_3$	-0.70 V	91.76	10	this work
CoTPP	0.5 M $KHCO_3$	-0.67 V	91	4	[1]
Co-salon	0.5 M $KHCO_3$	-0.70 V	75	10	[2]
CoPc@Fe-N-C	0.5 M KOH	-0.54 V	93	20	[3]
CoPc/CNT	0.1 M $KHCO_3$	-0.63 V	96	10	[4]
TTf-Por(Co)-COF	0.5 M $KHCO_3$	-0.70 V	95	10	[5]
COF-366-Co	0.5 M $KHCO_3$	-0.67 V	90	20	[6]
Co-N_5/HNPCSs	0.2 M $NaHCO_3$	-0.73 V	99.4	10	[7]

Experimental Details

Materials and General Methods. 1,8-Dihydroxynaphthalene (98%), sodium hydride (NaH, 60% dispersion in mineral oil), chloromethyl ethyl ether (95%), n-Butyllithium (2.5 mol/L in hexane), o-Phenylenediamine (98%), salicylaldehyde (98%), Cobalt (II) acetate tetrahydrate (98%), N,N,N′,N′-Tetramethylethylenediamine (99%) were purchased from Energy chemical. diethyl ether (anhydrous), dimethylformamide (DMF, anhydrous), ethyl acetate (EA) (99.5%), petroleum ether (PE) (99.5%), dichloromethane (DCM) (99.5%), 2-propanol (99.7%), mehtanol (99.5%), dimethyl sulfoxide (DMSO), ethanol (99.7%), hexane (97%), tetrahydrofuran (THF), hydrochloric acid (HCl, 12 mol/L), sodium chloride (NaCl, 99.9%), sodium sulfate (Na_2SO_4, 99%), potassium bicarbonate ($KHCO_3$,≥99.5%) were obtained from Sinopharm Chemical Reagent Co., Ltd. Toray TGP-H-060 carbon paper was purchased from Toray Industries Inc. Deionized water was used in all experiments.

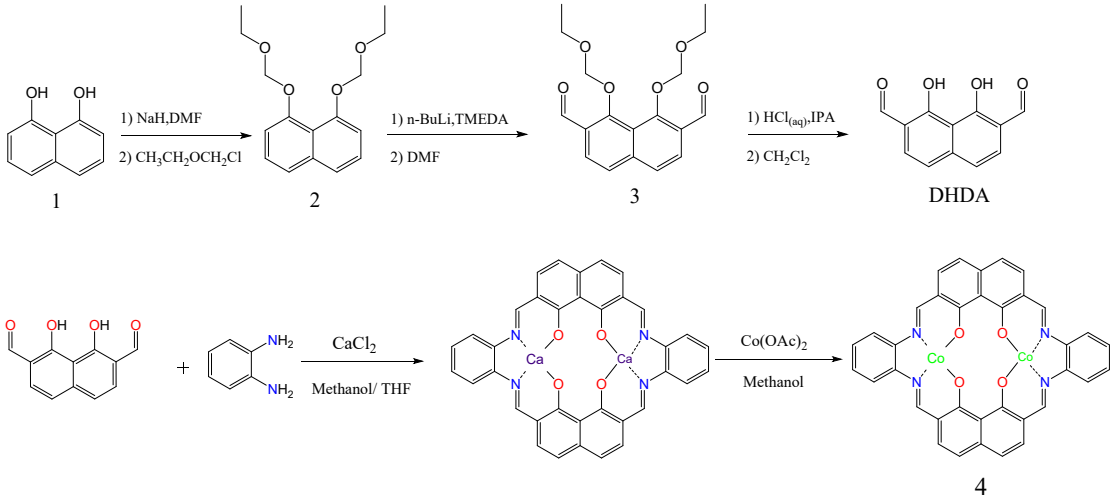

Scheme S1. The synthesis route of D-Co.

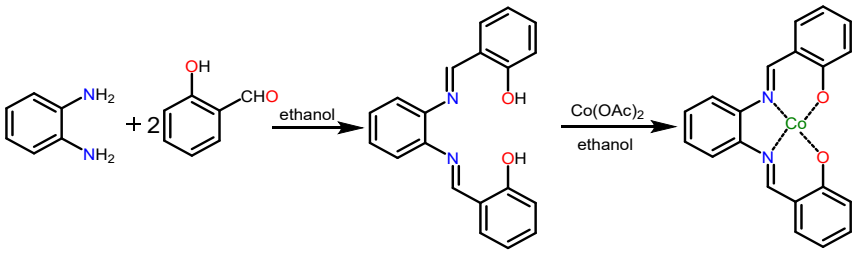

Scheme S2. Synthesis of Co-salophen (S-Co)

Synthesis of salophen (1).[8] salicylaldehyde (0.05 mol, 6.1 g) was added to a solution of 1,2-diaminobenzene (2.7 g, 0.025 mol) in 40 mL of ethanol. The contents were refluxed for 12 h. The product which was precipitated after cooling the reaction mixture, filtered and washed with cold ethanol. Finally the salophen compound was obtained by being dried under vacuum at 80 ℃ for overnight. ^{1}H NMR (400 MHz, DMSO): δ 12.92 (s, 2 H), 8.92 (s, 2H), 7.65 (d, J=7.6 Hz, 2H), 7.43 (m, J=9.2 Hz, 2H), 7.39 (m, J=9.2 Hz, 4H), 6.94 (t, J=16 Hz, 4H), ^{13}C NMR (100MHz, DMSO): δ 164.5, 160.8, 142.7, 133.9, 132.9, 128.2, 120.2, 119.9, 119.5, 117.1ppm. LCMS-QTOF: m/z 317.1269 ($M+H^{+}$).

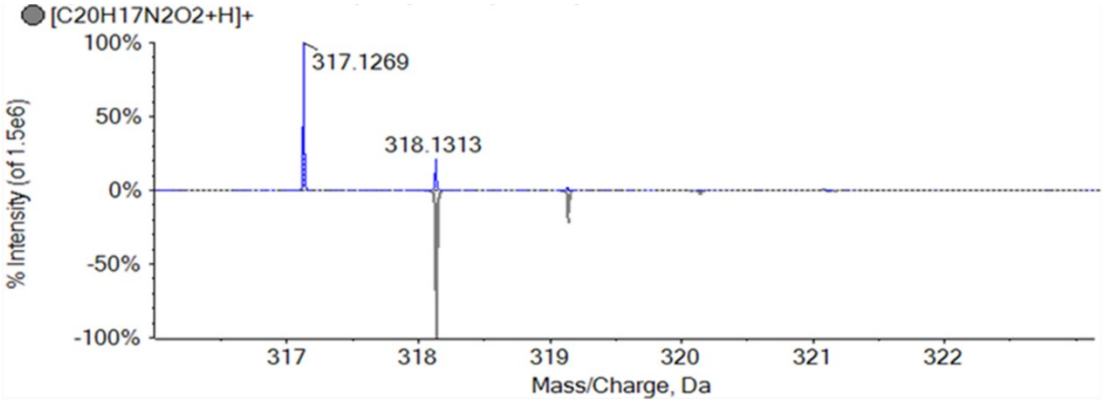

Fig. S1. LCMS-QTOF of salophen ($C_{20}H_{16}N_2O_2$).

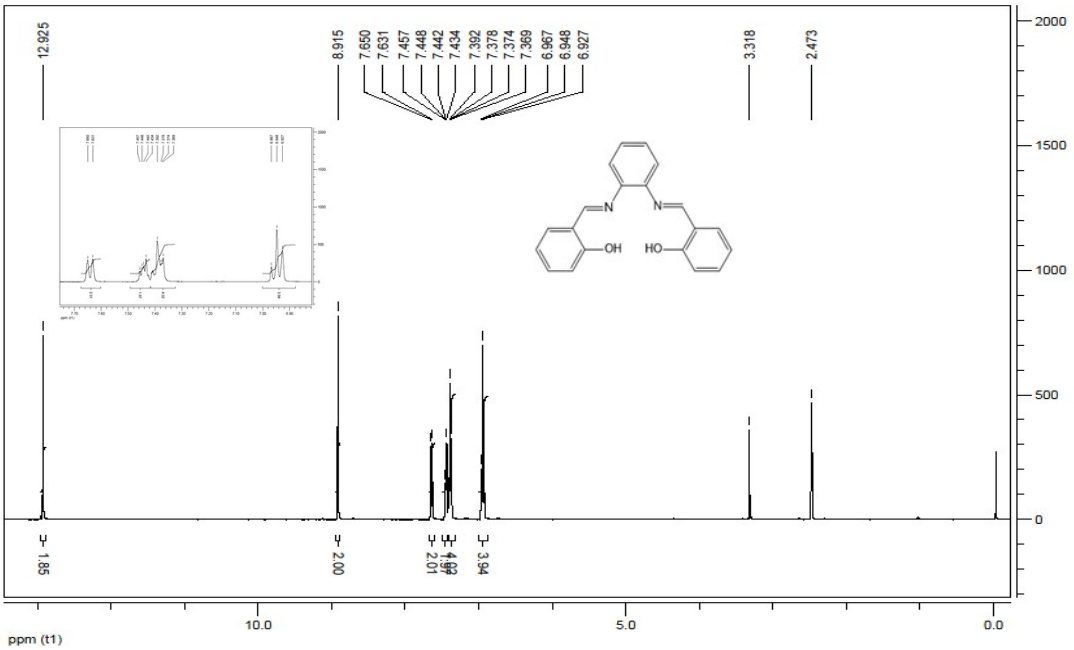

Fig. S2. ^{1}H NMR spectrum (DMSO, 400 MHz, 298 K) of salophen.

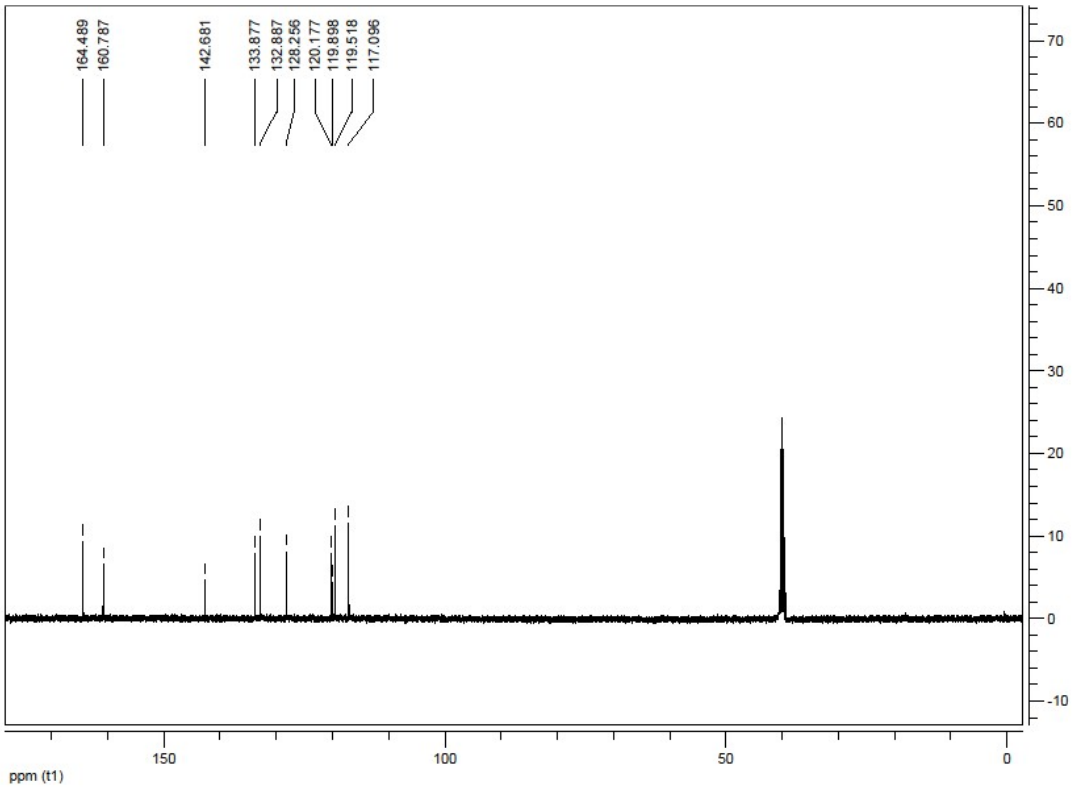

Fig. S3. ^{13}C NMR spectrum (DMSO, 100 MHz, 298 K) of salophen

Synthesis of Co-salophen (2).[9] In a typical synthesis of Co-salophen (S-Co), the mixture of salophen (0.632 g), $Co(CH_3COO)_2 \cdot 4H_2O$ (0.498 g) and ethanol (12 mL) was added to the inner tank of autoclave. The mixed solution was sonicated for 5 min and heated at 120℃ for 48 h. After the autoclave was naturally cooled to room temperature for 12 h, black crystals precipitated. The precipitation was washed with ethanol for several times and dried in vacuum at 80 ℃ for overnight. LCMS-QTOF: m/z 373.0400 ($M+H^+$). ICP-AES: calad. Co 15.84, found Co 15.92.

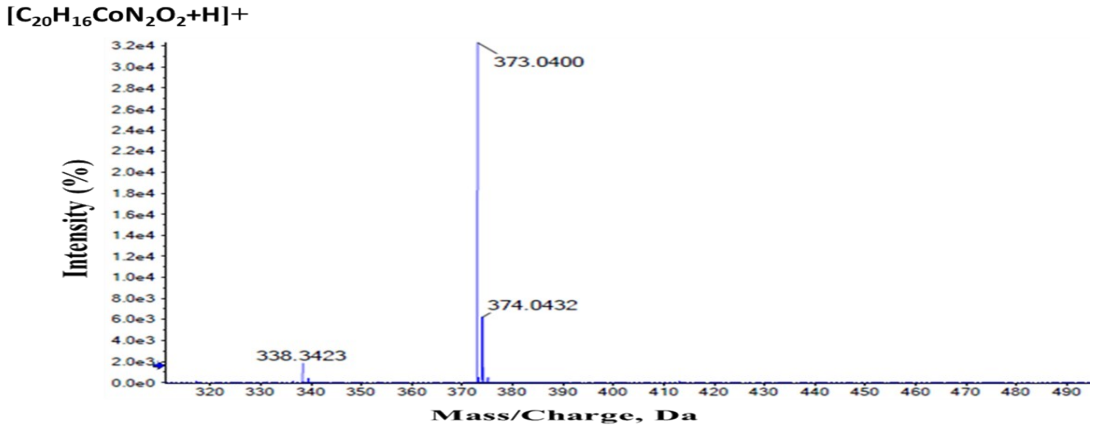

Fig. S4. LCMS-QTOF of S-Co ($C_{20}H_{16}CoN_2O_2$)

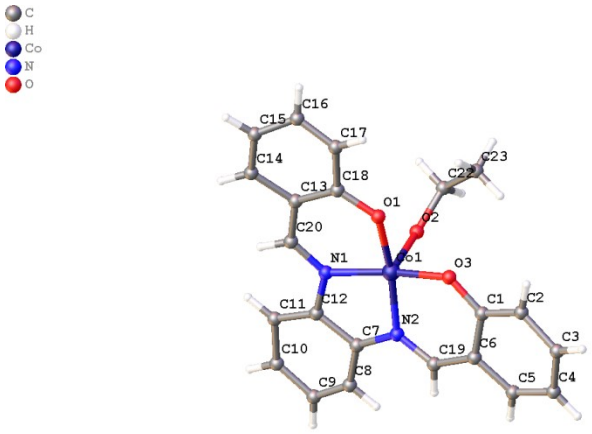

Fig. S5. The single-crystal structure of S-Co.

Table S2. Crystallographic data of S-Co.

Sample	**S-Co**
CCDC number	2205384
Empirical formula	$C_{22}H_{19}CoN_2O_3$
Formula weight	418.32
***T* [K]**	293
Crystal system	Orthorhombic
Space group	Pna21
***a* [Å]**	19.876(15)
***b* [Å]**	5.168 (3)
***c* [Å]**	18.265 (12)
***α* [°]**	90.000
***β* [°]**	90.000
***γ* [°]**	90.000
***V* [Å^3]**	1876.6(2)
Z	4
F(000)	864.0
Density [g/cm^3]	1.481
***μ* [mm^{-1}]**	0.940
Reflections collected	4572
Unique reflections	2766
***R* (int)**	0.0180
GOF	1.102
$R_1[I>2\sigma(I)]$	0.0537
$\omega R_2[I>2\sigma(I)]$	0. 1709
R_1**(all data)**	0.0772
ωR_2**(all data)**	0. 1566

Synthesis of 1,8-bis(ethoxymethoxy)naphthalene (2).[10] To a solution of naphthalene-1,8-diol (1) (1.60 g, 10 mmol) in DMF (15 mL) at 0 °C was added 60% NaH (1.2g, 30 mmol), DMF (15 mL) and stirred for 1 h. A solution of chloromethyl ethyl ether (2.8 mL, 30 mmol) in Et_2O (15 mL) was added to the mixture. After stirring overnight (0 °C to r.t), the reaction mixture was added to ice water (50 mL) and extracted with EA (30 mL × 3). The organic extracts were combined, dried over anhydrous Na_2SO_4, filtered and concentrated. The residue was purified using column chromatography on silica gel (PE/EA) to yield 2 (2.40 g, 87%) as a white liquid. ^{1}H NMR (400 MHz, $CDCl_3$): δ 7.37 (d, J= 7.2 Hz, 2 H), 7.23 (t, J = 8.0 Hz, 2 H), 7.00 (d, J = 8.4 Hz, 2 H), 5.23 (s, 4 H), 3.75 (q, 4 H), 1.17 (t, 6 H), ^{13}C NMR (100 MHz, $CDCl_3$): δ 152.7, 136.4, 125.1, 121.5, 118.2, 111.4, 94.0, 63.4, 14.1 ppm. LCMS-QTOF: m/z 277.1409 ($M+H^+$).

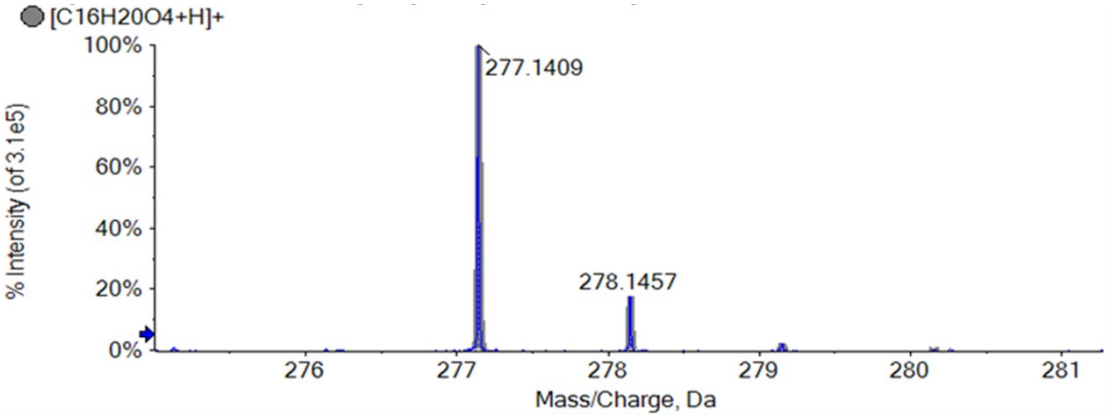

Fig. S6. LCMS-QTOF of 1,8-bis(ethoxymethoxy)naphthalene.

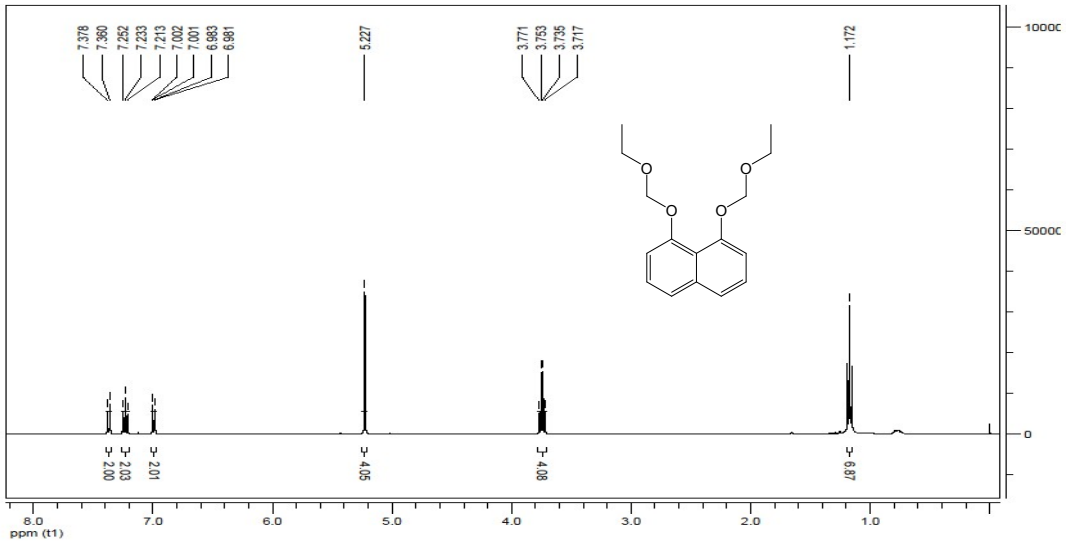

Fig. S7.^{1}H NMR spectrum ($CDCl_3$, 400 MHz, 298 K) of 1,8-bis(ethoxymethoxy) -naphthalene

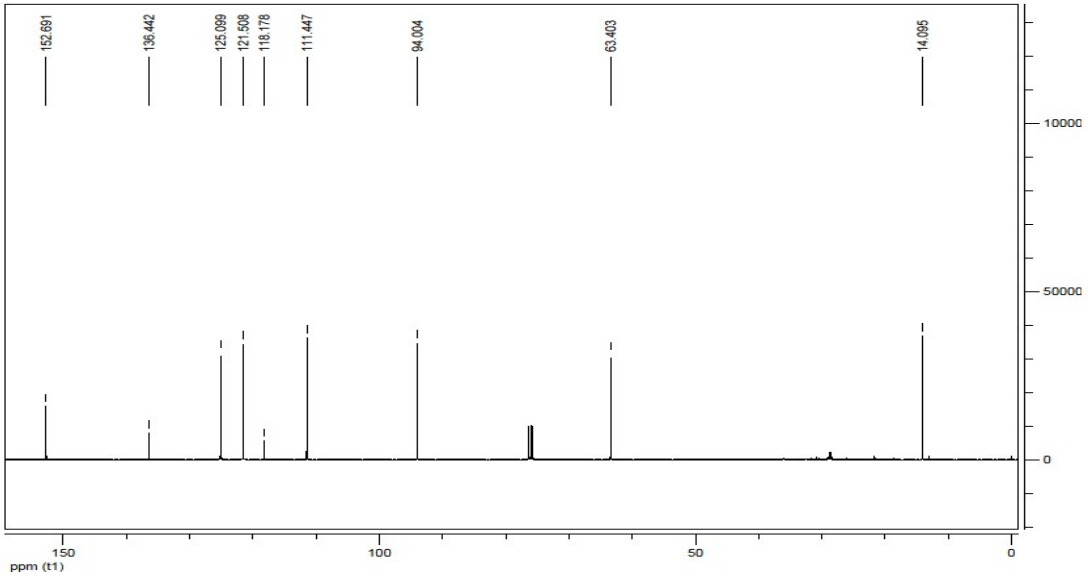

Fig. S8. ^{13}C NMR spectrum ($CDCl_3$, 100 MHz, 298K) of 1,8-bis(ethoxymethoxy)naphthalene.

Synthesis of 1,8-bis(ethoxymethoxy)naphthalene-2,7-dicarbalde-hyde (3). Under the protection of nitrogen, a solution of compound 2 (3.0 g, 11 mmol) and Et_2O (70 mL) at 0°C was added dropwise to a mixture of n-BuLi (2.5 M in hexane, 13.2 mL, 33 mmol) and TMEDA (5.0 mL, 33 mmol) in Et_2O (45 mL) and stirred for 6 h at 0 °C. DMF (5.2 mL, 66 mmol) was added to the mixture for stirring overnight (0 °C to r.t). Water (40 mL) was added to the mixture and the pH 7 adjusted using 1.0 M HCl (aq.). After extracted with EA, the organic layer was dried over Na_2SO_4, filtered and evaporated. The residue was purified using column chromatography on silica gel (PE/EA) to yield the 3 (2.21 g, 61%) as an ochre solid. ^1H NMR (400 MHz, $CDCl_3$): δ 10.60 (s, 2 H), 8.02(d, J = 8.4 Hz, 2 H), 7.72 (d, J = 8.4 Hz, 2 H), 5.29 (s, 4 H), 3.83 (q, 4 H), 1.22 (t, 6H). ^{13}C NMR (100 MHz, $CDCl_3$): δ 190.3, 159.0, 143.5, 128.4, 126.0, 125.8, 121.4, 100.8, 66.8, 15.0ppm. LCMS-QTOF: m/z

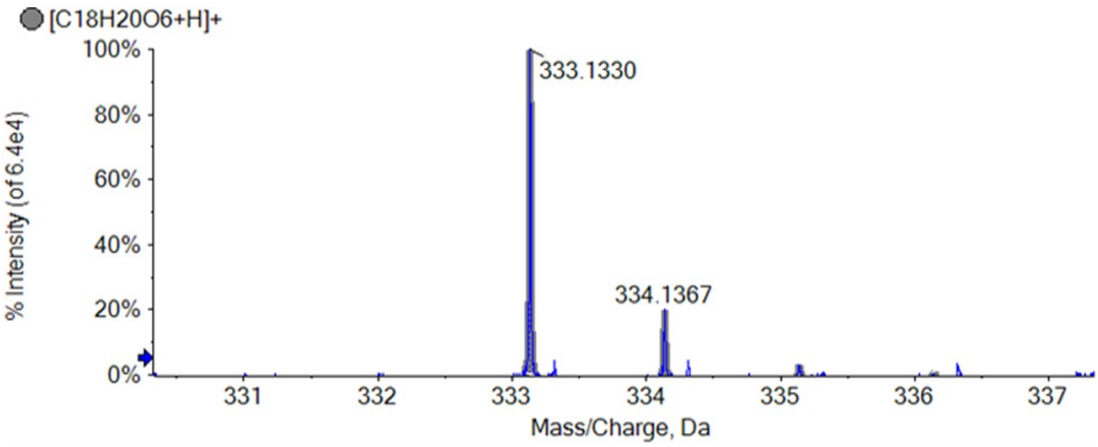

333.1330 ($M+H^+$).

Fig. S9. LCMS-QTOF of 1,8-bis(ethoxy-methoxy) naphthalene-2,7-dicarbalde-hyde.

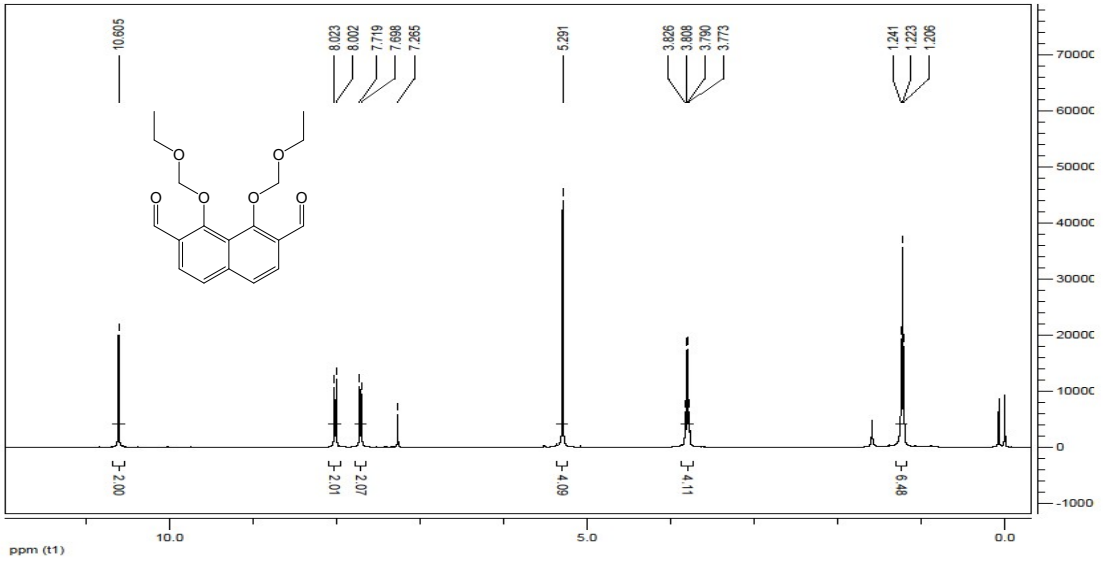

Fig. S10. ^{1}H NMR spectrum ($CDCl_3$, 400 MHz, 298 K) of 1,8-bis(ethoxy- methoxy)naphthalene- 2,7-dicarbalde-hyde.

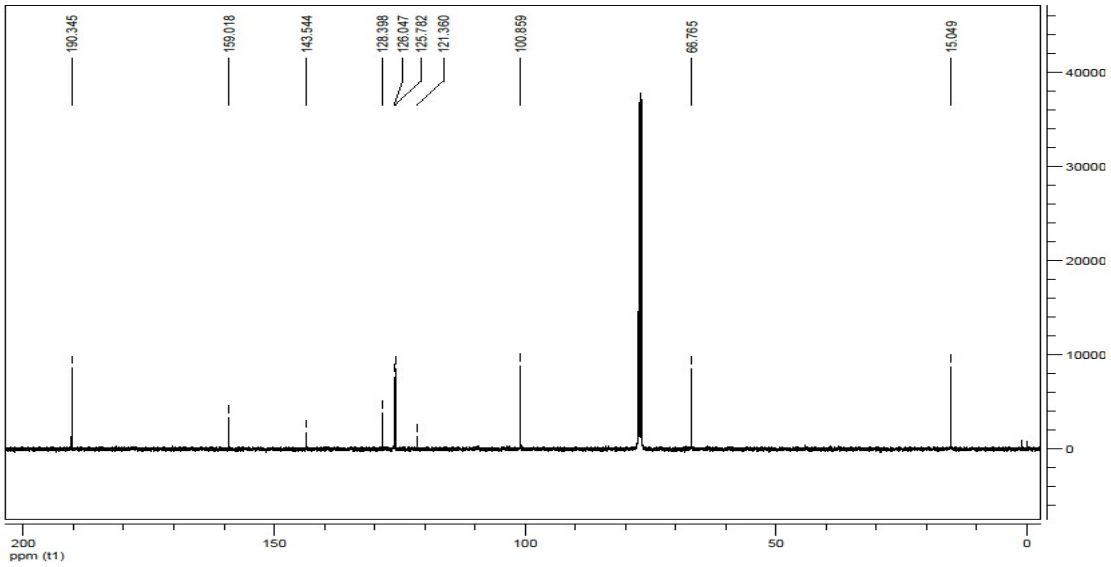

Fig. S11. ^{13}C NMR spectrum ($CDCl_3$, 100 MHz, 298 K) of 1,8-bis(ethoxy- methoxy)naphthalene- 2,7-dicarbalde-hyde.

S**ynthesis of 1,8-dihydroxynaphthalene-2,7-dicarbaldehyde (DHDA).** Under the protection of nitrogen, a solution of compound 3 (1.25 g, 4.1 mmol) in CH_2Cl_2 (70 mL) at 0 °C was added dropwise to a mixture of isopropanol (30 mL) and HCl (7.5 mL). After stirring for 2 h at this temperature. After stirring overnight (0 °C to r.t), the reaction mixture was added to water (50 mL). The mixture was extracted with CH_2Cl_2, dried over anhydrous Na_2SO_4, filtered and evaporated. The residue was purified using column chromatography on silica gel (PE/DCM) to yield the DHDA (0.60 g, 69%) as a yellow solid. ^{1}H NMR (400 MHz, $CDCl_3$): 10.16 (s, 2 H), 7.75 (d, J = 8.0 Hz, 2 H), 7.32 (d, J = 8.4 Hz, 2 H).^{13}C NMR (100 MHz, $CDCl_3$) δ 193.4, 164.2, 143.0, 130.4, 119.9, 116.4, 113.9ppm. LCMS-QTOF: m/z 217.0470 ($M+H^+$).

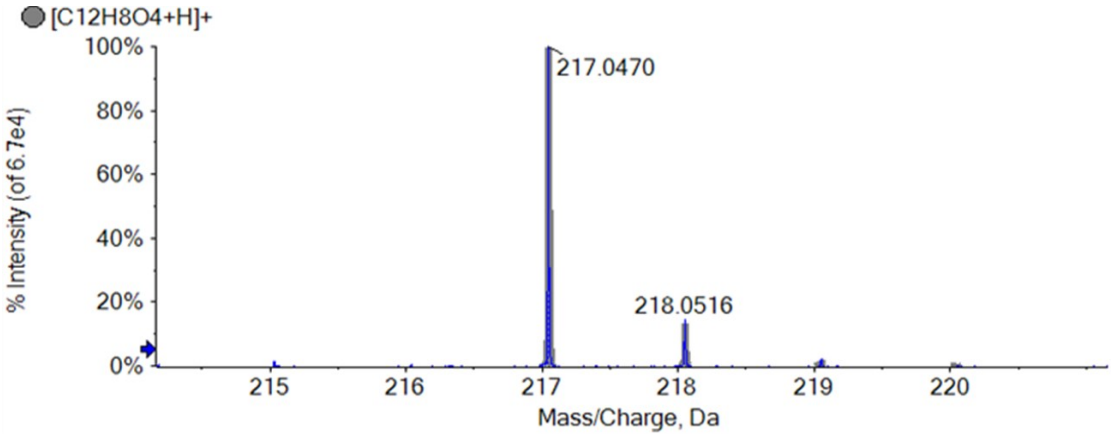

Fig. S12. LCMS-QTOF of DHDA

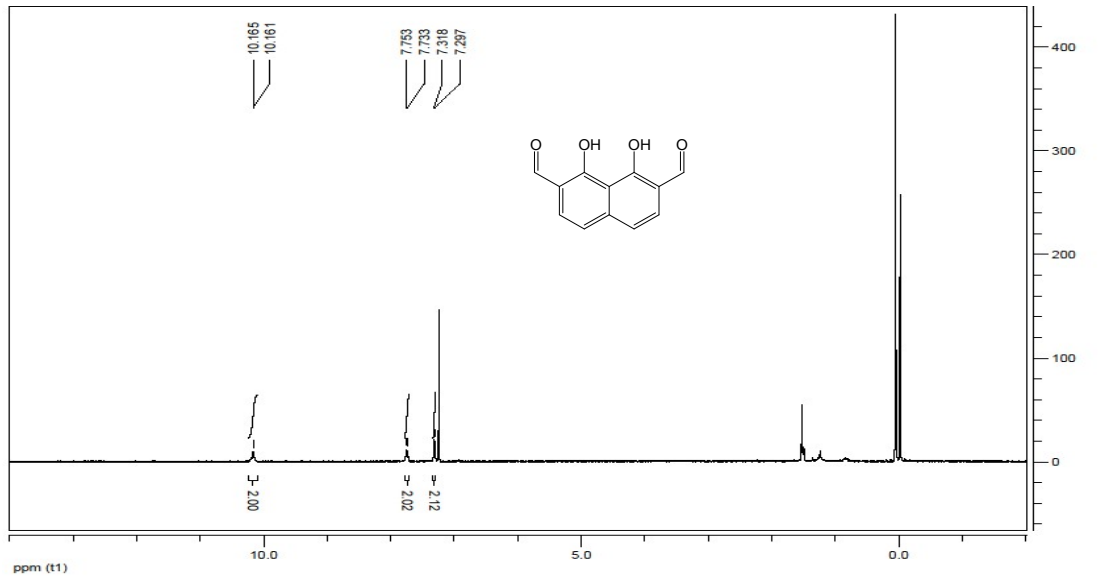

Fig. S13. ^{1}H NMR spectrum ($CDCl_3$, 400 MHz, 298 K) of DHDA.

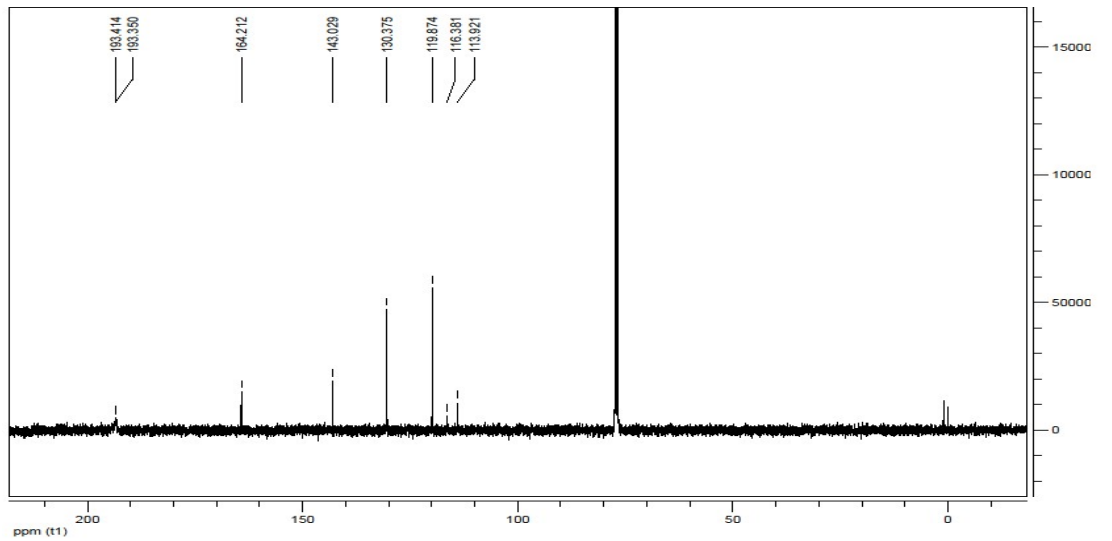

Fig. S14. ^{13}C NMR spectrum ($CDCl_3$, 100 MHz, 298 K) of DHDA.

Synthesis of 2Co-salophen (5).[11] Under the protection of nitrogen, DHDA (216 mg, 1mmol) in tetrahydrofuran (THF) (10 ml) was added slowly with stirring to *o*-phenylenediamine (108 mg, 1 mmol) and $CaCl_2$ (112 mg, 1mmol) in methanol (10 ml) and the mixture was heated at reflux for 5 h. The solution was allowed to cool and the precipitate of 2Ca-salophen was collected by filtration and washed with methanol then hot-water. A Pyrex tube measuring 10×8 mm was charged with 2Ca-salophen (65.2 mg, 0.1 mmol), Cobalt (II) acetate tetrahydrate (49.9 mg, 0.2 mmol), methanol (4 mL). The mixture solution was sonicated for 2 min at room temperature, degassed through three freeze-pump-thaw cycles, sealed under vacuum, heated at 100 ℃ for 48 h. After the mixture was naturally cooled to room temperature. The precipitates were washed with ethanol for several times, collected by filtration to afford 2Co-salophen as black solid, and dried in vacuum at 80 ℃ for overnight. LCMS-QTOF: m/z 691.0225 ($M+H^+$). ICP-AES: calad. Co 17.08, found Co 17.15.

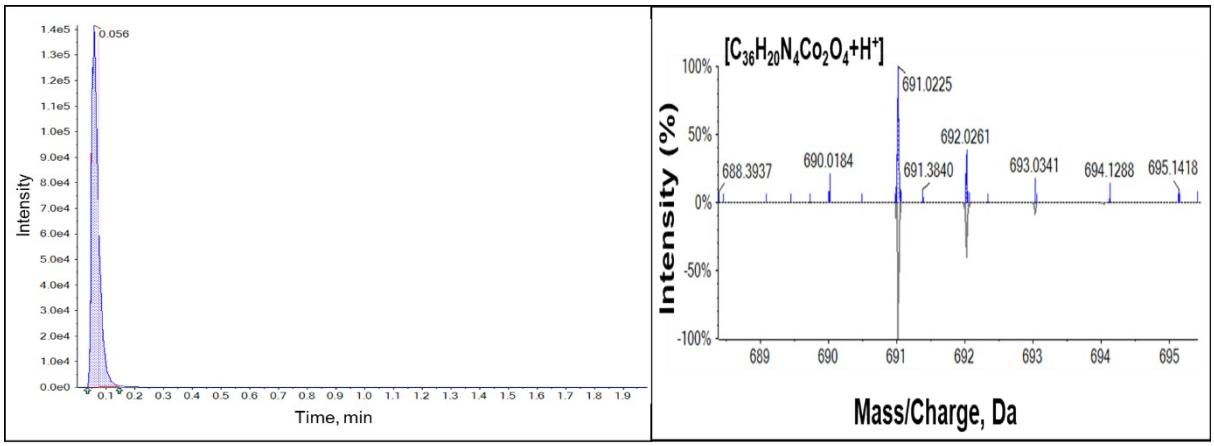

Fig. S15. LCMS-QTOF of 2Co-salophen ($C_{36}H_{20}Co_2N_4O_4$).

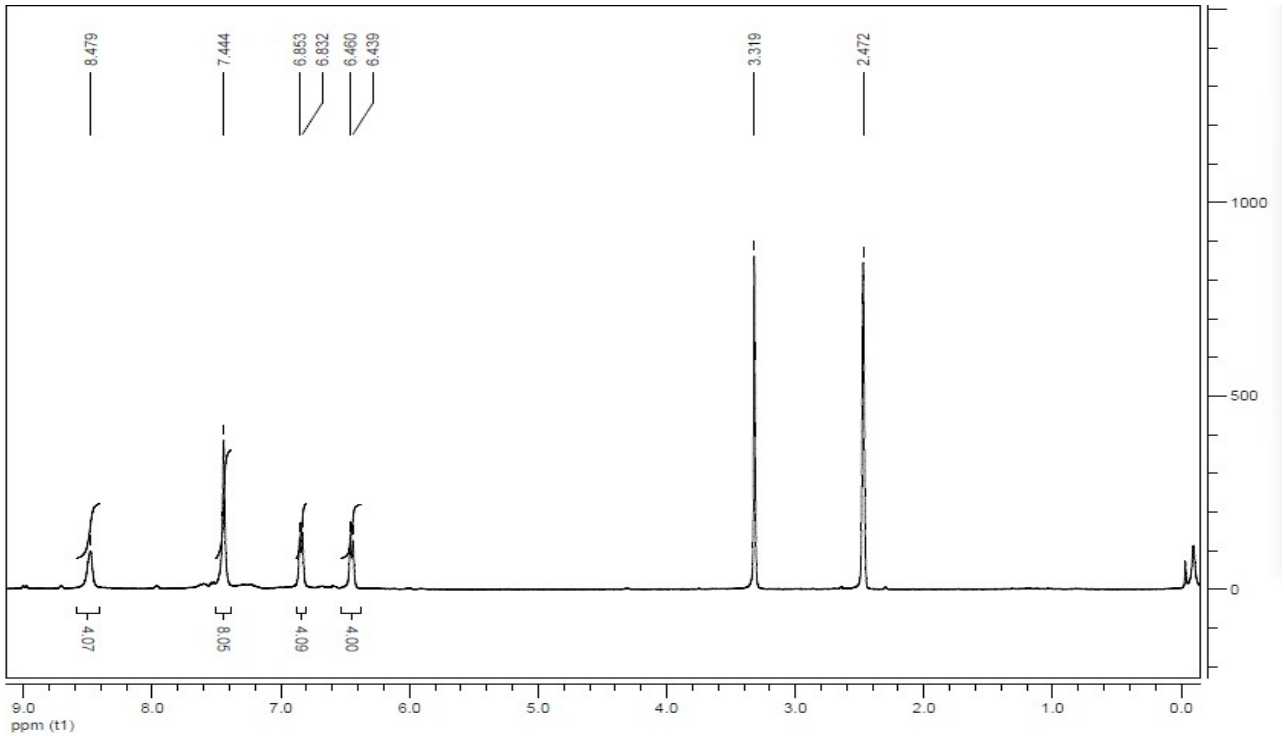

Fig. S16. ^{1}H NMR spectrum (DMSO, 400 MHz, 298 K) of 2Ca-Salophen ($C_{36}H_{20}Ca_2N_4O_4$)

Preparation of D-Co /CNT hybrid materials [12]

The CNTs were first calcined in a tube furnace at 500 °C in air for 5 h. After cooling to room temperature, the CNTs were transferred into a 5% HCl aqueous solution and sonicated for 1 h. The purified CNTs were collected by vacuum filtration, transfer to beaker and washed with deionized water under stirring and sonicating for three times until neutral, and then dried in vacuum at 100 °C overnight. The 15 mg D-Co （10 mg, 12mg, 15mg, 17mg and 20mg） was dissolved in 60 mL of DMSO, then 50 mg of the purified CNTs were added and dispersed with sonicate 1 h. The mixture was further stirred at room temperature for 20 h. Subsequently, the mixture was filtered and the precipitate was washed with DMSO and ethanol. Finally, the precipitate was dried in vacuum at 120 °C overnight to yield the final product (D-Co/CNT). The S-Co was dissolved in CH_2Cl_2, the remaining steps were similar to the previous sample fabrication. The weight percentage of Cobalt in the hybrid material was ~3.94% for D-Co/CNT material, as confirmed by ICP-AES measurement.

Physicochemical characterizations

The morphology and composition of the catalysts were investigated using a scanning electron microscope (Hitachi S-4300 SEM) equipped with energy dispersive X-ray spectrometer (EDX). Transmission electron microscopy (TEM), High-angle annular dark-field scanning transmission electron microscopy (HAADF-STEM). X-ray photoelectron spectra (XPS) were recorded by a Thermo Scientific ESCALB 250Xi spectrometer with an Al Kα X-ray source and 1486.6eV pass energy. Usually, all binding energies calibrated by 284.8 eV of adventitious carbon contamination (C 1s), except carbon materials. When the samples are carbon materials which are labelled, they are calibrated by 284.4 eV, except the graphene is calibrated by 284 eV. ^{1}H NMR and ^{13}C NMR spectra were measured on a Bruker AVANCE 400 spectrometer in DMSO-d_6 (δ=2.50 ppm) and $CDCl_3$ (δ=7.26 ppm) using TMS as an internal standard. Mass spectra were obtained with X500R QTOF spectrometers. The Raman spectra were obtained by means of a Renishaw (INVIA) confocal Raman microscope with a 785 nm laser. The infrared absorption spectra were measured on a Bruker TENSOR Ⅱ using KBr as an internal standard.

Electrochemical measurements

Working electrode preparation

5.0 mg of hybrid materials (D-Co/CNT) were dispersed into 2.5 mL ethanol and 50 μL Nafion solution, followed by sonication for 1 h to achieve a homogeneous ink. Next, 800 μL of the catalyst ink was uniformly spread onto a carbon fiber paper (Toray 060) with the area of 1×1 cm^2 (catalyst mass loading, 0.8 mg cm^{-2}). The prepared electrode was used as the working electrode.

Electrochemical measurements

All the electrochemical measurements were performed in a gas-tight H-type electrochemical cell with two-compartments, the cathode and anode compartments were separated by a cation-exchange membrane (Nafion 117). The graphite rod and saturated Ag/AgCl were used as counter and reference electrodes, respectively. The CO_2 (99.999%) was continuously bubbled into the catholyte during electrolysis at a flow rate of 20 sccm per minute using a calibrated mass flow controller. All CO_2 reduction experiments were performed in CO_2-saturated 0.5 M $KHCO_3$ aqueous solution at room temperature (298 K) and ambient condition. After CO_2 was injected into 0.5 M $KHCO_3$ solution for at least 30 min, controlled potential electrolysis was performed at each potential for 1h. The potentials were controlled by an Autolab potentiostat/galvanostat (CHI 760E). All potentials were measured against the Ag/AgCl reference electrode and converted to the reversible hydrogen electrode (RHE) reference scale on account of the equation: E (*vs* RHE) = E (*vs* Ag/AgCl) +0.197V+0.0591×pH. The gas products of electrocatalysis were analyzed using an online GC equipped with TCD and FID detector, the liquid products were quantified after electrocatalysis using ^{1}H NMR with solvent (D_2O) suppression. 300 μl of electrolyte was mixed with 200 μl D_2O and 2 μl dimethyl sulfoxide (DMSO) as internal standards for the ^{1}H NMR analysis. No liquid product was detected.

The linear sweep voltammetry (LSV) curves of the two Co-based molecular catalysts were performed in CO_2-saturated 0.5M $KHCO_3$ at the scan rate of 10 mV s^{-1}.

The cyclic voltammetry (CV) curves of the two catalysts were measured at various scan rates (10, 20, 40, 60, 80, and 100 mV s^{-1}) and non-faradaic current under CO_2 atmosphere to obtain the double layer capacitance (C_{dl}).

The electrochemical impedance spectra (EIS) of the catalysts were recorded with AC voltage with 5 mV amplitude at open circuit potential within the frequency range from 0.01 Hz to 100 KHz.

Calculation of Faradaic Efficiency (FE)

$$FE_{CO} = \frac{2Fv_{CO}GP}{RT\ i_{total}} \times 100\%$$

Calculations were performed based on the definition of faradaic efficiency (FE):[13]

Where 2 is the number of electrons required to produce one CO molecule; F is the faradaic constant (96485 C mol^{-1}); v_{CO} is the volume ratio of product CO obtained from GC; G is the volumetric flow rate (20 sccm); P is atmospheric pressure (101.3 Kpa); R is the ideal gas constant (8.314 J $mol\ K^{-1}$); and T is the sample loop temperature (298 K).

Turnover frequency (TOF) for CO production was calculated as follow:

The TOF (h^{-1}) of product CO was evaluated as follows:[14]

$$TOF = \frac{I_{product}/NF}{m_{cat} \times w/M_{metal}} \times 3600$$

Where $I_{product}$ is the partial current for certain product, CO; N is the number of electrons transferred for CO production, which is 2 for CO; F is the faradaic constant (96485 C mol^{-1}); m_{cat} is the mass of catalyst on the electrode, g; w is the metal loading in the catalyst based on ICP-AES results; Mmetal is the atomic mass of Co (58.93 g mol^{-1}).

Computational method

The plane-wave code Vienna Ab-initio Simulation Package (VASP) was applied for all the first principal calculations with using projector augmented-wave pseudopotentials with the PBE functional.41-42 A model with periodic boundary conditions was used and the plane wave energy cutoff was set to 400 eV. The sample the reciprocal space for all calculation systems is Monkhorst-Pack k-point grid of 3 × 3 × 2. To prevent the interaction between the replicas along the z-direction, at least 20 Å vacuum spaces were used between adjacent images.

The adsorption energy was calculated by the following equation:

$$E_a = E_{final} - E_{substrate} - E_{adsorbate}$$

where E_a, E_{final}, $E_{substrate}$ and $E_{adsorbate}$ are the adsorption energy of adsorbate on substrate, total energy of adsorbate on this substrate, total energy of substrate, and total energy of adsorbate.

The free energy of this reaction was calculated by following equation: $\Delta G = E_a + \Delta ZPE - T\Delta S$

where ΔG, ΔZPE and ΔS represent Gibbs free energy, zero-point energy and the entropy, respectively.

The reaction paths for CO_2 electroreduction to CO are known to encompass the following seven elementary steps:

$CO_2 + * \rightarrow CO_2*$ (1)

$H_2O + * \rightarrow H_2O*$ (2)

$H_2O* + H^+ \rightarrow H_3O^{*+}$ (3)

$CO_2* + H_3O^{*+} + e^- \rightarrow COOH* + H_2O*$ (4)

$H_2O* + H^+ \rightarrow H_3O^{*+}$ (5)

$COOH* + H_3O^{*+} + e^- \rightarrow CO* + H_2O*$ (rate-determining step) (6)

$CO* \rightarrow CO + *$ (7)

Where * denotes active sites on the catalyst surface.

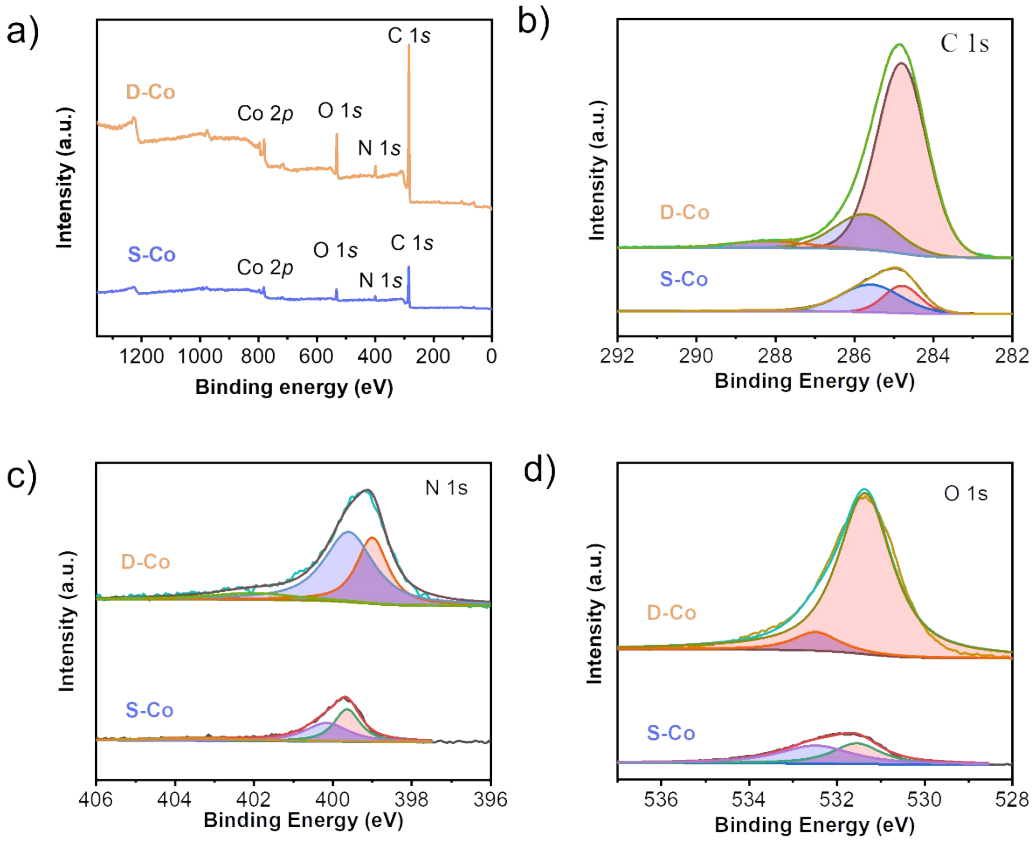

Fig. S17. a) XPS spectra of the survey scan for D-Co and S-Co. b), c), d) High-resolution XPS C1s, N1s, O1s spectrum of D-Co and S-Co.

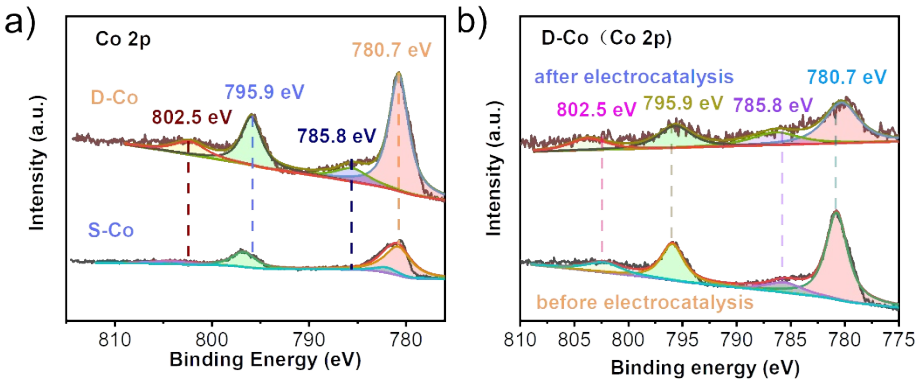

Fig. S18. a) High-resolution XPS Co 2p spectrum of samples. b) High-resolution XPS Co 2p spectrum of the D-Co both before and after electrocatalysis.

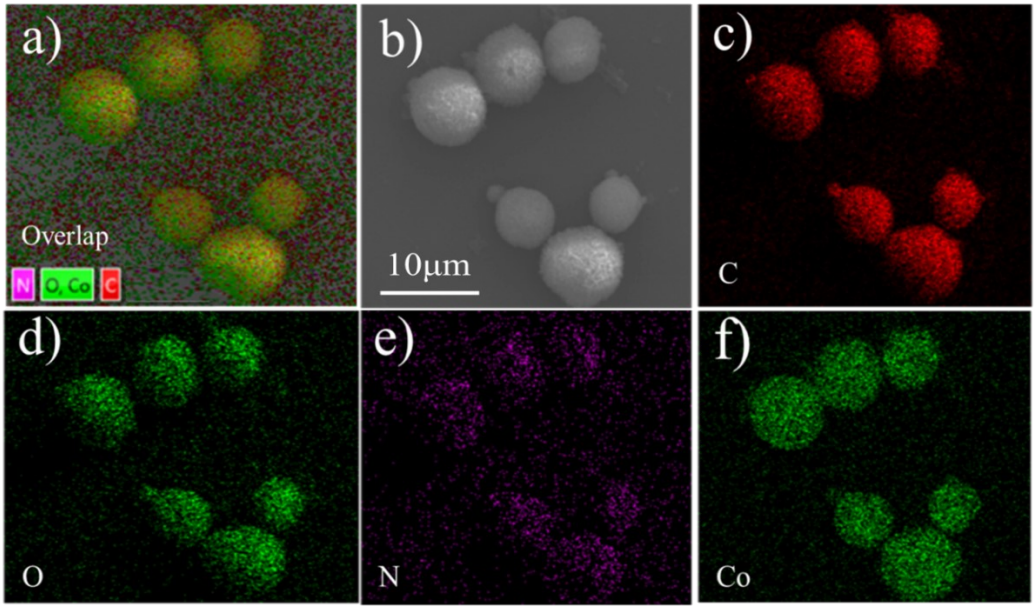

Fig. S19. EDS images of D-Co.

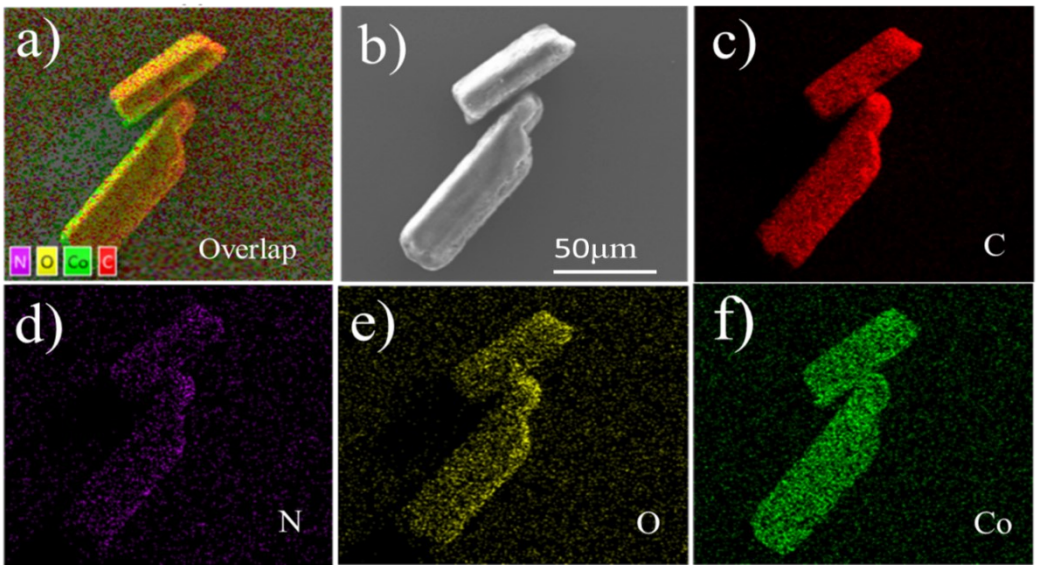

Fig. S20. EDS images of S-Co.

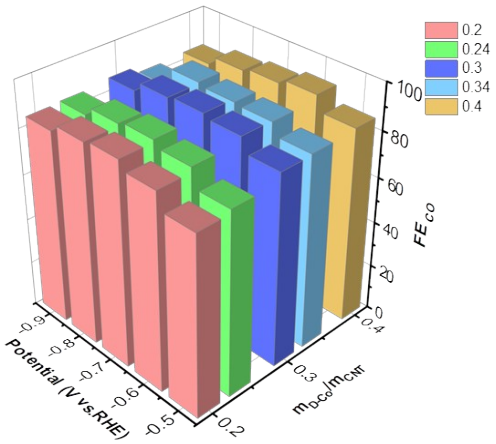

Fig. S21. 3D bar graph of potentials, the ratio of catalyst to CNT mass and FE_{CO}.

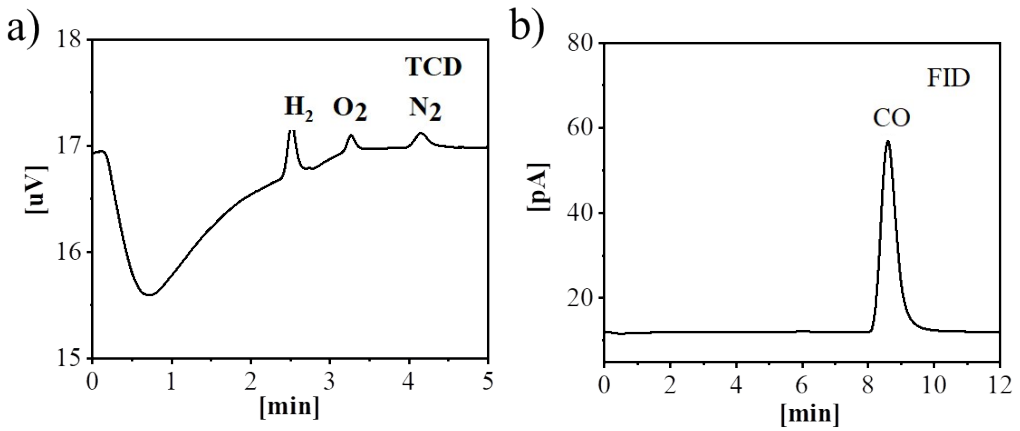

Fig. S22. GC analysis of gas products for D-Co/CNT in the CO2-saturated 0.5 M KHCO3 electrolyte during constant potential electrolysis.

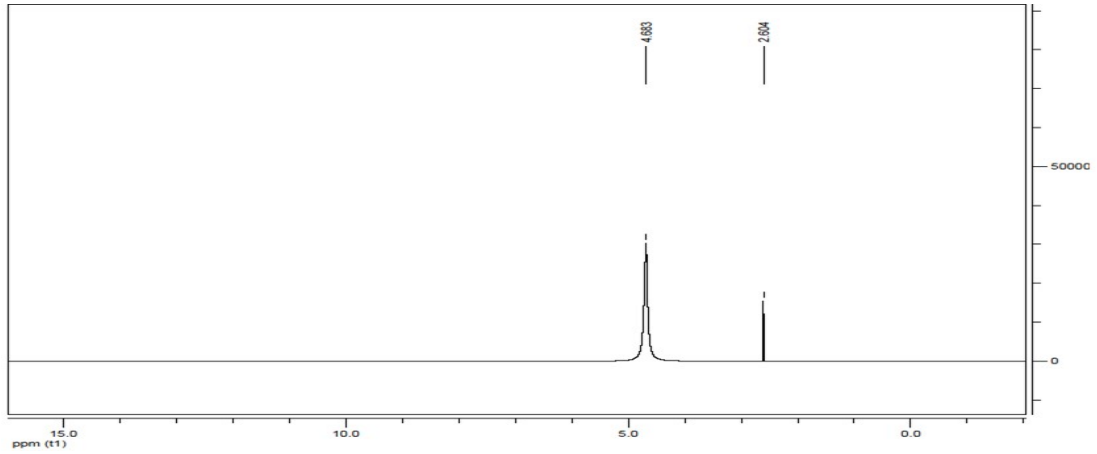

Fig. S23. ^{1}H NMR results of liquid product of D-Co/CNT in the CO_2-saturated 0.5 M $KHCO_3$ electrolyte after constant potential electrolysis.

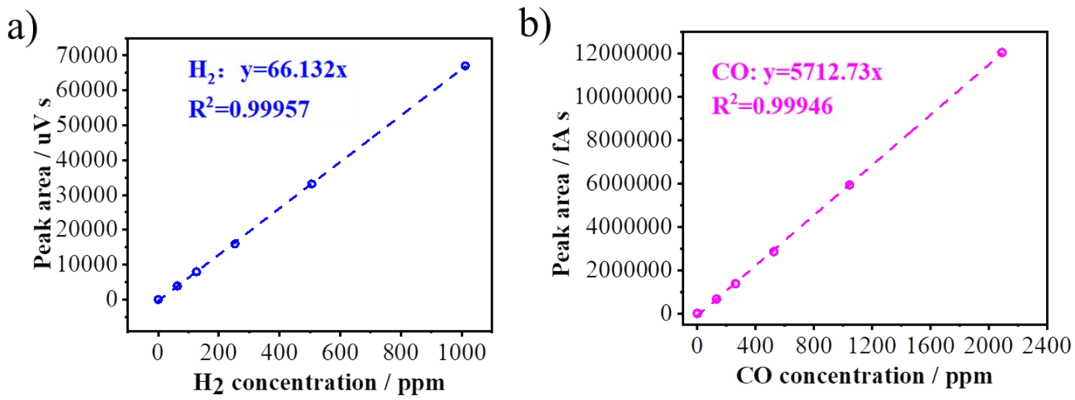

Fig. S24. GC calibration curves. (a) GC calibration curves for H_2. (b) GC calibration curves for CO.

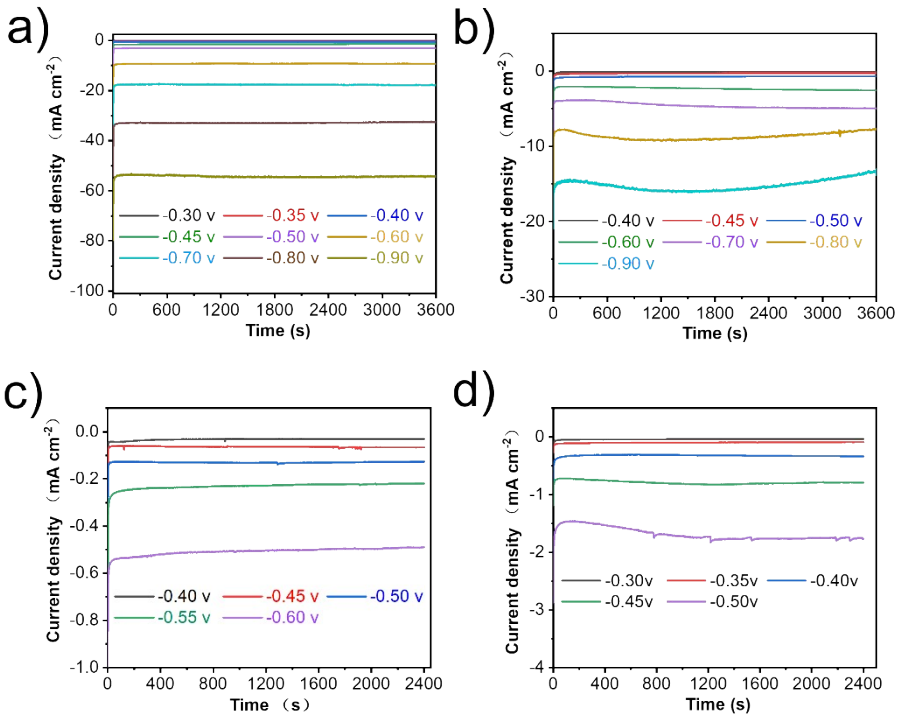

Fig. S25. 3600 seconds continuous chronoamperometric experiments for CO_2RR at different applied potentials on a) D-Co/CNT, b) S-Co/CNT; 2400 seconds continuous chronoamperometric experiments for CO_2RR at different applied potentials on c) CNT, d) D-Co.

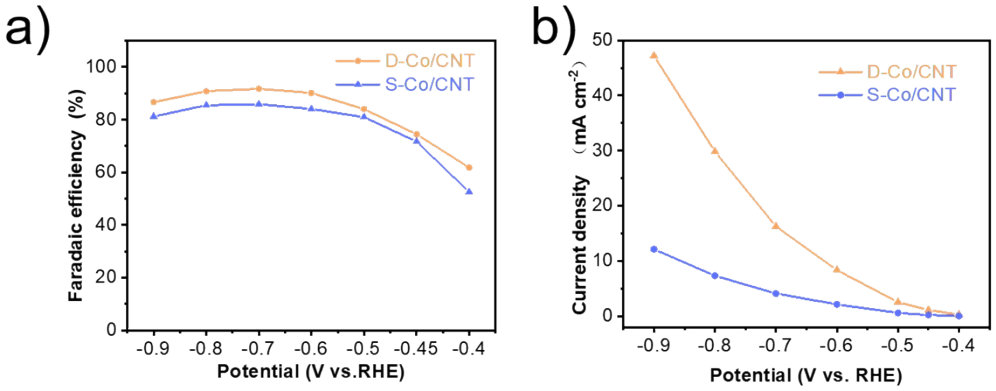

Fig. S26. a) FE_{CO} and b) J_{CO} of S-Co/CNT, D-Co/CNT.

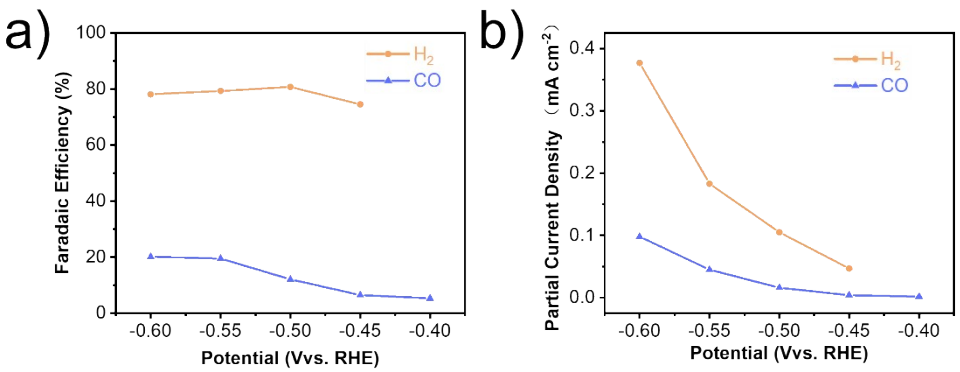

Fig. S27. a) FE and b) partial current density of CNT.

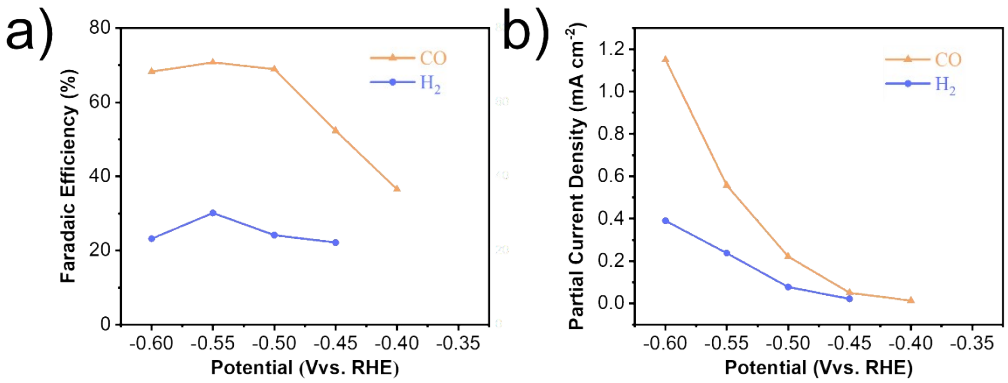

Fig. S28. a) FE and b) partial current density of D-Co.

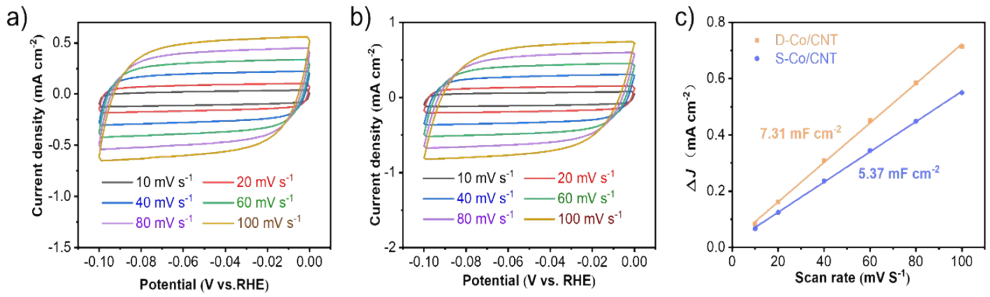

Fig. S29. CV curves with varied scan rate for a) S-Co/CNT and b) D-Co/CNT. c) The capacitive current plotted as a function of scan rate of D-Co/CNT and S-Co/CNT.

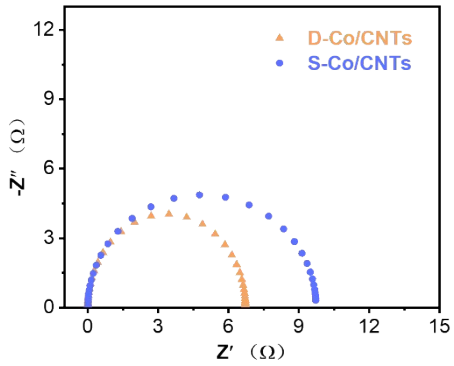

Fig. S30. Nyquist plots of different electrocatalysts.

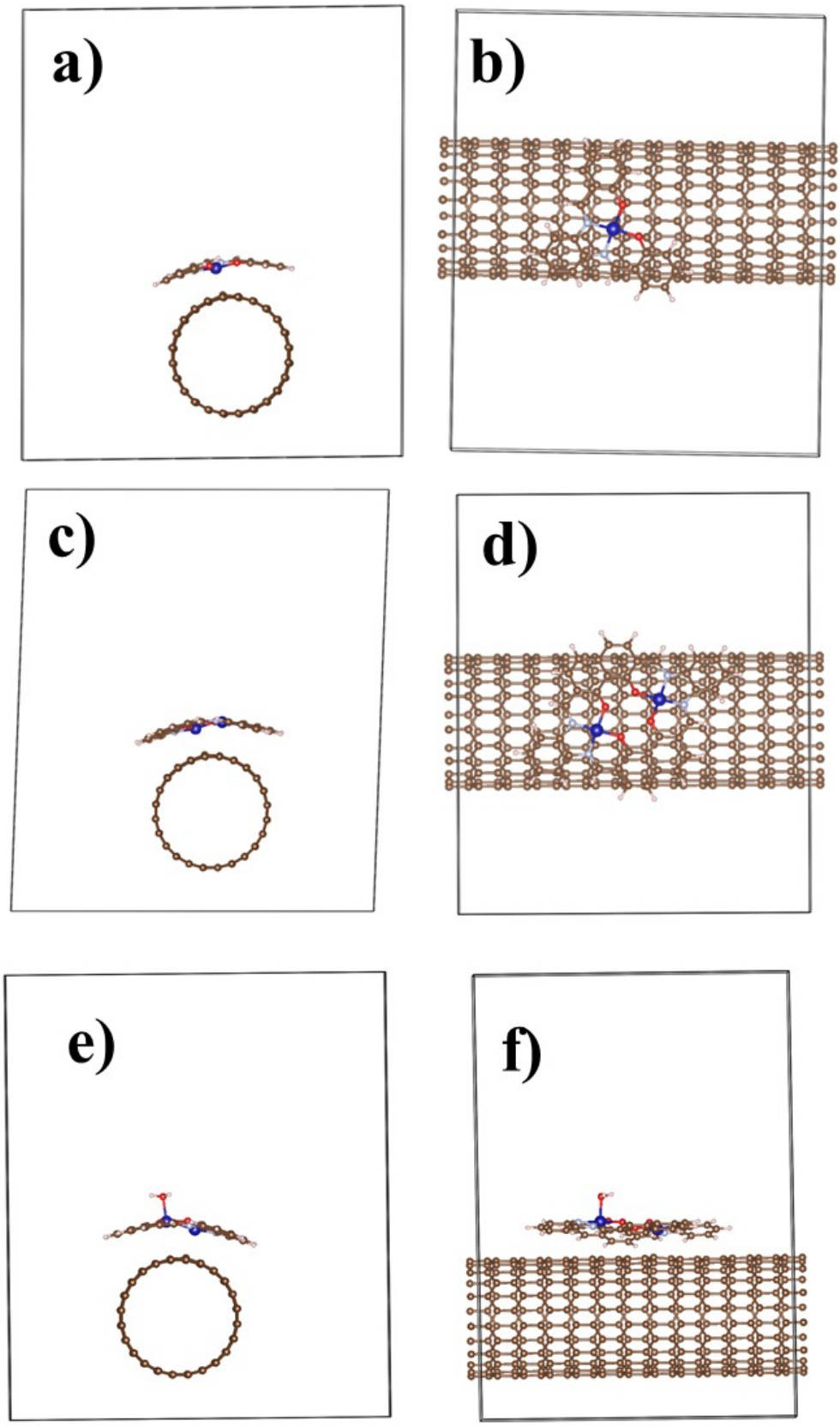

Fig. S31. The calculation models of S-Co/CNT, D-Co/CNT and H_2O-D-Co/CNT (left: side view; right: top view).

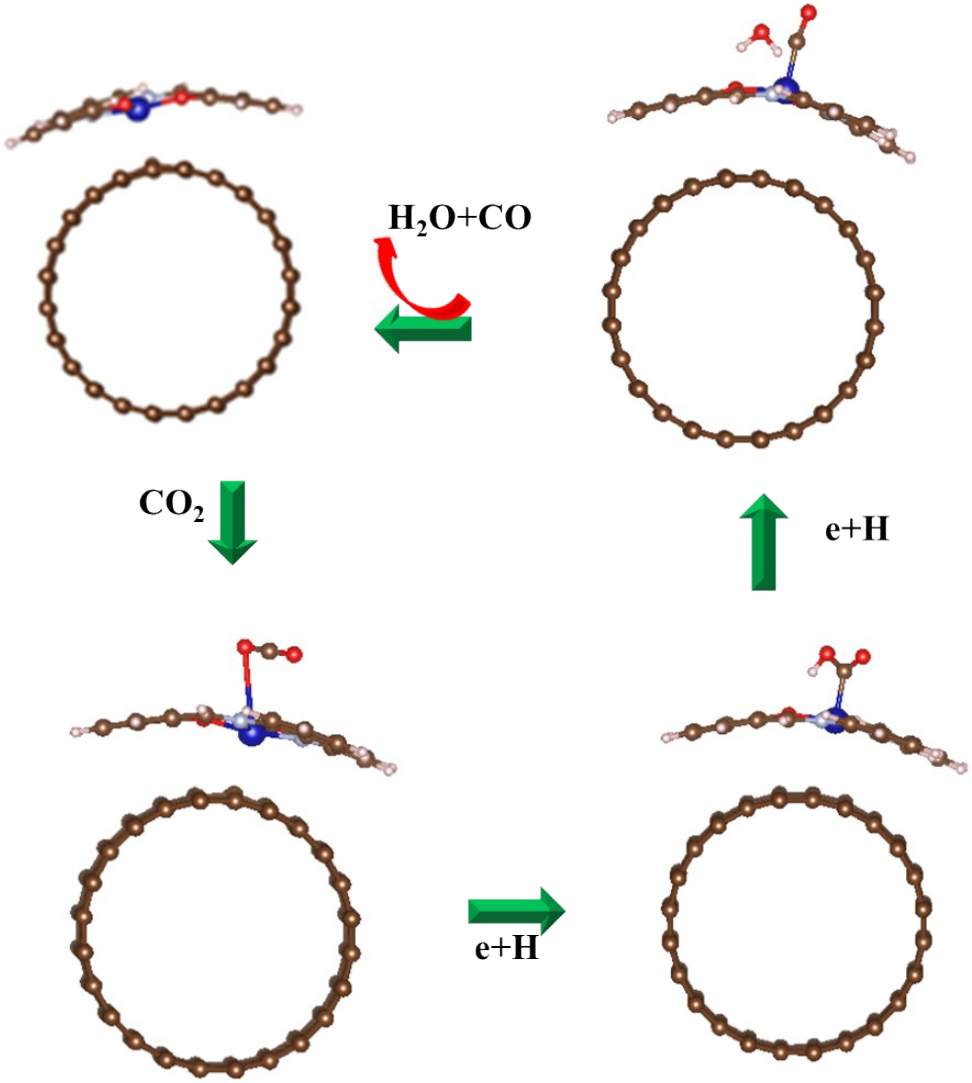

Fig. S32. The calculated CO_2RR mechanism catalyzed by S-Co/CNT.

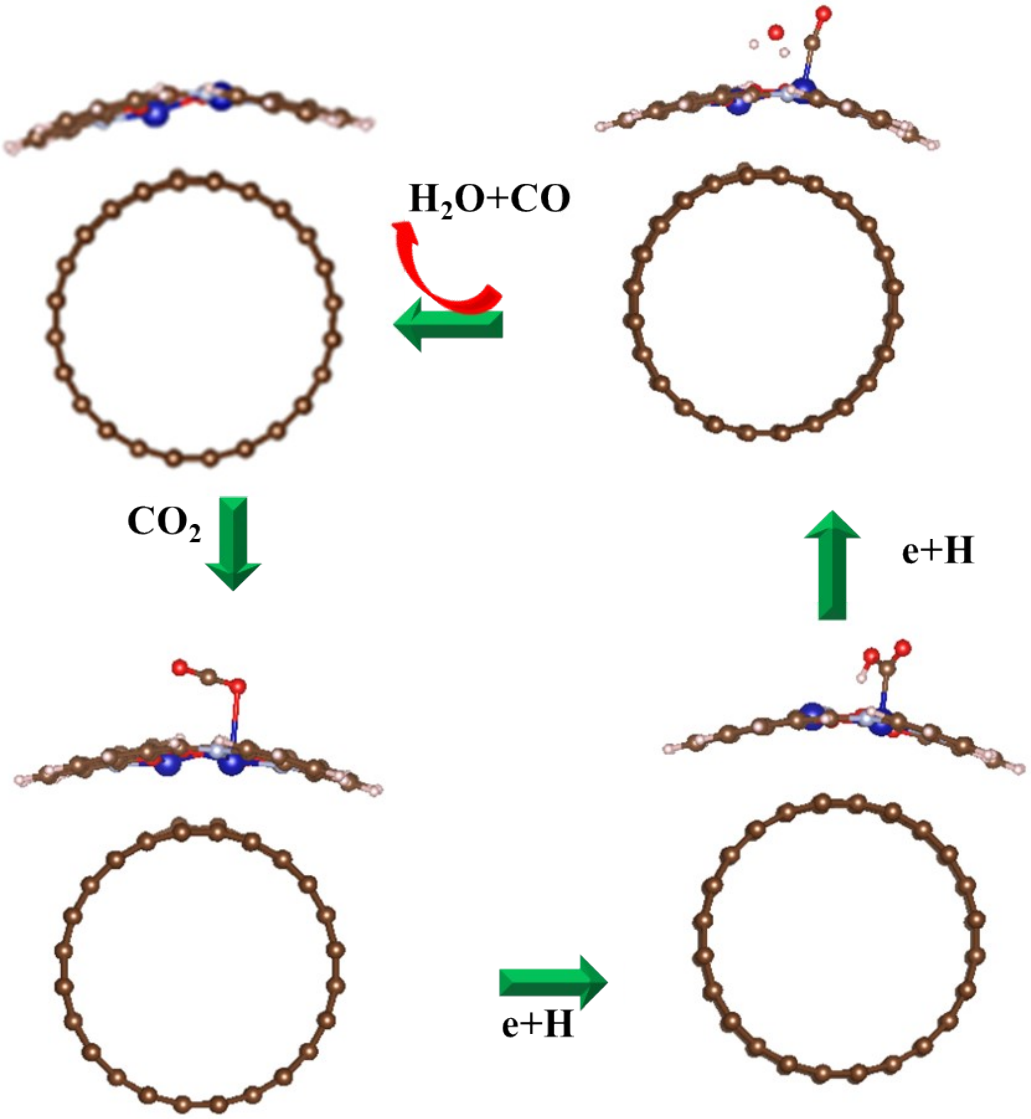

Fig. S33. The calculated CO_2RR mechanism catalyzed by D-Co/CNT.

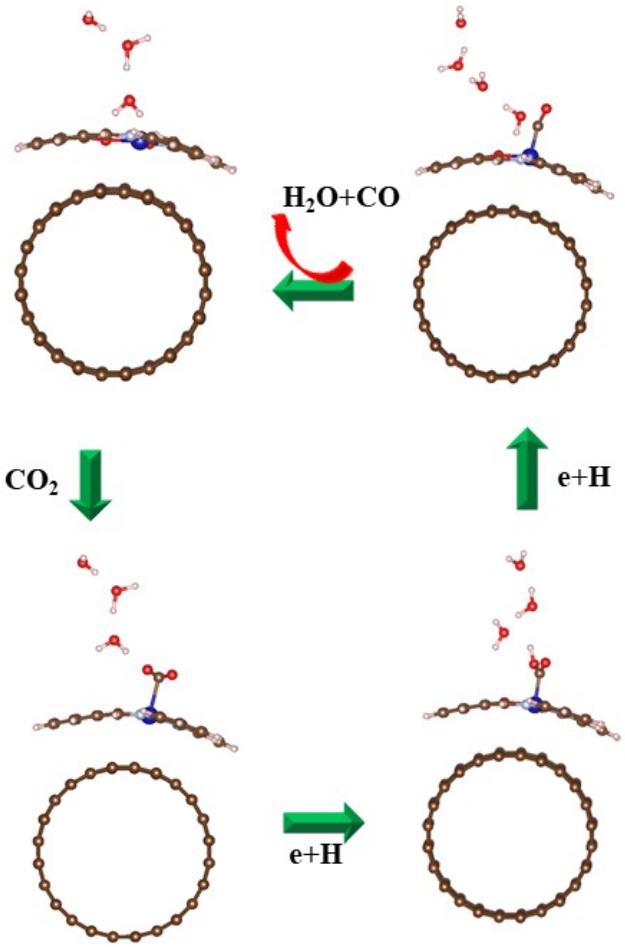

Fig. S34. The calculated CO_2RR mechanism catalyzed by $3H_2O$-D-Co/CNT.

Table S3. The adsorption energy of CO_2 and H_2O at Co site in three calculational catalysis models.

	S-Co /CNT	D-Co /CNT	H_2O-D-Co /CNT
adsorption energy/CO_2	0.341	0.836	0.966
adsorption energy/H_2O	1.059	1.246	0.759
C=O bond length	1.173	1.174	1.164

References

[1] X. -M. Hu, M. H. Rønne, S. U. Pedersen, T. Skrydstrup, K. Daasbjerg, *Angew. Chem. Int. Ed.,* 2017, 56, 6468-6472.

[2] X. Kong, Y. Liu, P. Li, J. Ke, Z. Liu, F. Ahmad, W. Yan, Z. Li, Z. Geng, J. Zeng, *Applied Catalysis B: Environmental*, 2020, 268, 118452.

[3] L. Lin, H. Li, C. Yan, H. Li, R.Si, M. Li, J. Xiao, G. Wang, X. Bao, *Adv. Mater.,* 2019, 31, 1903470.

[4] X. Zhang, Z. Wu, X. Zhang, L. Li, Y. Li, H. Xu, X. Li, X. Yu, Z. Zhang, Y. Liang, H. Wang, *Nature Communications*, 2017, 8, 14675.

[5] Q. Wu, R.-K. Xie, M.-J. Mao, G.-L. Chai, J.-D. Yi, S.-S. Zhao, Y.-B. Huang, R. Cao, *ACS Energy Lett.,* 2020, 5, 1005-1012.

[6] S. Lin, C. S. Diercks, Y.-B. Zhang, N. Kornienko, E. M. Nichols, Y. Zhao, A. R. Paris, D. Kim, P. Yang, O. M. Yahi, C. J. Chang, *Science*, 2015, 349, 6253, 1208-1213.

[7] Y. Pan, R. Lin, Y. Chen, S. Liu, W. Zhu, X. Cao, W. Chen, K. Wu, W.-C. Cheong, Y. Wang, L. Zheng, J. Luo, Y. Lin, Y. Liu, C. Liu, J. Li, Q. Lu, X. Chen, D. Wang, Q. Peng, C. Chen, Y. Li, *J. Am. Chem. Soc.,* 2018, 140, 4218-4221.

[8] Li, N.; Wang, Y.; Liu, F.; Zhao, X.; Xu, X.; An, Q.; Yun, K. Air-stable zirconium (IV)-salophen perfluorooctanesulfonate as a highly efficient and reusable catalyst for the synthesis of 3,4-dihydropyrimidin-2-(1H)-ones/thiones under solvent-free conditions. *Appl Organomental Chem.* 2019; 34: e5454.

[9] N. Li, Y. Wang, F. Liu, X. Zhao, X. Xu, Q. An, K. Yun, *Appl Organomental Chem.,* 2020; 34: e5454.

[10] Y. -T. Chen, P.-J. Wu, C.-Y. Peng, J.-Y. Shen, C.-C. Tsai, W.-P. Hu, P.-T. Chou, *Phys. Chem.Chem. Phys.*, 2017, 19, 28641.

[11] Z. -L. Yuan, Q.-L. Zhang, X. Liang, B.-X. Zhu, L. F. Lindoy, G.Wei, *Polyhedron*, 2008, 27, 344-348.

[12] Y. Wu, Z. Jiang, X. Lu, Y. Liang, H. Wang, *Nature.,* 2019, 575, 639-642.

[13] W. Xie, H. Li, G. Cui, J. Li, Y. Song, S. Li, X. Zhang, J. Lee, M. Shao, M. Wei, *Angew. Chem. Int. Ed.,* 2021, 60, 7382-7388.

[14] W. Ren, X. Tan, W. Tan, W. Yang, C. Jia, S. Xu, K. Wang, S. C. Smith, C. Zhao, *Angew. Chem. Int. Ed.,* 2019, 58, 1-6.